Heart HIF-1α and MAP Kinases During Hypoxia: Are They Associated *In Vivo*?

ANNA CARETTI,*,[1] SANDRINE MOREL,†,[1] GIUSEPPINA MILANO,† MONICA FANTACCI,* PAOLA BIANCIARDI,* RAFFAELLA RONCHI,* GIUSEPPE VASSALLI,† LUDWIG K. VON SEGESSER,† AND MICHELE SAMAJA*,[2]

**Department of Medicine, Surgery, and Dentistry, University of Milan, San Paolo Hospital, Milan I-20142, Italy; and †Centre Hospitalier Universitaire Vaudois, 1005 Lausanne, Switzerland*

To study the *in vivo* dynamics of hypoxia-inducible factor 1α (HIF-1α), master regulator of O_2-dependent gene expression, and mitogen-activated protein kinases (MAPKs) in the hypoxic myocardium, Sprague-Dawley rats (n = 4 to 6 per group) were exposed to 1-hr hypoxia (10% O_2), 23-hr hypoxia, and 23-hr hypoxia, followed by reoxygenation. HIF-1α increased 15-fold after 1-hr hypoxia, remained constant for 23 hrs, and returned to baseline on reoxygenation. Extracellular signal–regulated kinases (ERK1/2) were unchanged throughout. Phosphorylated p38 increased 4-fold after 1-hr hypoxia and returned to baseline within 23-hr hypoxia. The activity of stress-activated protein kinases/c-Jun NH_2-terminal kinases (JNKs), measured as phosphorylated c-Jun, increased 3-fold after 1-hr hypoxia and remained sustained afterward. Furthermore, HIF-1α was halved in rats that were administered with the p38 inhibitor SB202190 and made hypoxic for 1 hr. In conclusion, although very sensitive to the reoxygenation, HIF-1α is overexpressed *in vivo* in the hypoxic myocardium, and its acute induction by hypoxia is correlated with that of p38. Exp Biol Med 232:887–894, 2007

Key words: p38; JNK; ERK1/2; SB202190; c-Jun; HSP27

Introduction

Inadequate O_2 supply with respect to needs, or hypoxia, elicits a variety of physiologic, metabolic, and molecular responses in whole organisms, tissues, and cells. The α subunit of the hypoxia-inducible factor 1 (HIF-1α) plays a pivotal role in orchestrating the cell responses to hypoxia. In the absence of O_2, HIF-1α stabilization allows formation of a supramolecular complex (1), which binds to cognate responsive elements on DNA and regulates the transcription of more than 500 downstream genes (2). The presence of O_2 destabilizes HIF-1α *via* hydroxylation of two proline residues by specific prolyl hydroxylases, which targets HIF-1α to proteasomal degradation, thereby preventing DNA binding (3). The value for the Michaelis-Menten constant for O_2 in the proline hydroxylation reaction is greater than arterial PO_2 (4), suggesting that prolyl hydroxylases are effective O_2 sensors and that HIF-1α is activated even during normoxia, which has been confirmed by experimental evidence (5). The lack of a clear threshold of hypoxia for HIF-1α activation also would suggest the possible occurrence of parallel regulators of the O_2 sensing mechanism such as, for example, mitogen-activated protein kinases (MAPKs). Three major MAPK cascades are recognized in eukaryotes: the extracellular signal-regulated kinases 1 and 2 (ERK1/2), stress-activated protein kinases/c-Jun NH_2-terminal kinases 1 and 2 (JNK), and p38. These pathways independently regulate a variety of cell mechanisms, including cell growth and differentiation (ERK1/2) and apoptosis (p38 and JNK). In Hep3B and HEK293 cells, the hypoxia response involves Rho family small GTPase Rac1, a critical determinant of intracellular redox status that activates p38 (6). In addition, genetic evidence supports a role for p38 in HIF-1α activation, because mouse embryonic fibroblast *p38*$\alpha^{-/-}$ cells, as well as cells deficient in Mkk3 and Mkk6, upstream regulators of p38α, which is one of the four known isoforms of p38 MAPK, fail to activate HIF-1α in hypoxia (7). However, an *in vivo* validation of p38-mediated activation of HIF-1α is still lacking.

The purposes of this study are: (1) to investigate the dynamics of HIF-1α during *in vivo* hypoxia in the myocardium, a situation for which there is little support for HIF-1α overexpression, and (2) to test the association between MAPK and HIF-1α *in vivo*. To these aims, we

This study was supported in part by the Italian Ministry of University and Research (PRIN Projects 2004).

[1] These authors contributed equally to the study.

[2] To whom correspondence should be addressed at University of Milan, San Paolo Hospital, via di Rudinì 8, I-20142 Milan, Italy. E-mail: Michele.Samaja@unimi.it

Received January 30, 2007.
Accepted March 19, 2007.

1535-3702/07/2327-0887$15.00

exposed rats to normobaric hypoxia (10% O_2) for up to 23 hrs, followed by reoxygenation and measured MAPK protein expression, phosphorylation, and activity, as well as HIF-1α expression. To start examining a cause-effect relationship *in vivo*, we also tested whether this association still occurred after selective inhibition of p38 action (8).

Materials and Methods

Animals. The investigation conformed to the Guide for the Care and Use of Laboratory Animals published by the National Institutes of Health (NIH publication no. 85–23, revised 1996). Male Sprague-Dawley rats (5 wks of age, 230–250 g body wt at entry into the study) were purchased from IFFA-Credo (L'Arbresle, France). All animals had free access to water and conventional laboratory diet until 24 hrs before the experiment. Room temperature was kept at 21°C ± 2°C, and 12 hrs of light were automatically alternated to 12 hrs of dark. To induce hypoxia, rats were exposed to an atmosphere containing 10% O_2, balance N_2, whereas the control normoxic animals were kept for 23 hrs in a cage flowed with room air ($n = 6$). The other groups were: 1-hr hypoxia ($n = 6$), 23-hr hypoxia ($n = 6$), and 23-hr hypoxia followed by 1-hr reoxygenation ($n = 4$). To test the effect of selective inhibition of p38, an additional group of animals ($n = 4$) were injected subcutaneously just before hypoxia (1 hr) with 1 mg/ml per kg of 4-(4-fluorophenyl)-2-(4-hydroxyphenyl)-5-(4-pyridyl)1H-imidazole (SB202190; Calbiochem, San Diego, CA), a potent, selective cell-permeable p38 inhibitor with reported $IC_{50} = 50$ n*M* and no effect on ERK1/2 or JNK activity.

At the end of the treatments, animals were transferred anaerobically one at a time into a procedure chamber kept at the same $\%O_2$ content as the hypoxic chamber, anesthetized by intraperitoneal injection of Na-thiopental (10 mg/100 g body wt) plus heparin (500 units), and sacrificed by cervical dislocation. After sacrifice the animals were taken out of the chamber, had the thorax quickly opened and the heart was removed, immersed in liquid nitrogen (<0.5 min after sacrifice), and finally stored at –80°C until analysis, by a procedure that minimizes HIF-1α degradation (9–11).

HIF-1α Immunohistochemistry. Biopsies from frozen myocardium tissue were processed to obtain serial 5-μm–thick sections that were placed on silanized glass slides and used for HIF-1α immunoperoxidase and immunofluorescence as described (9, 11). Immunoperoxidase slides were examined at ×40 magnification in a microscope (Axiolab E; Carl Zeiss, Göttingen, Germany), whereas immunofluorescence slides were examined at the same magnification in an inverted fluorescence microscope (Axiovert 25 CFL; Carl Zeiss) equipped with a filter for detection of fluorescein (filter set 09, excitation band pass 450–490 nm, emission low pass 515 nm). In both cases, randomly chosen images were acquired by a CCD camera (AxioCam czv CD 4.0; Carl Zeiss) and stored in a PC.

The algorithm used for HIF-1α quantification includes quantitative immunohistochemistry by calculating the cumulative signal strength, or energy, of the digital file representing the image. The algorithm involves subtracting the energy of the digital file encoding the control image (i.e., not exposed to antibody) from that of the experimental image (i.e., antibody treated) to calculate the absolute amount of antibody-specific chromogen per pixel. The images were analyzed by IPlab Software (Scanalytics Inc., Billerica, MA) and split into RGB channels. The green channel was used to calculate the color intensity as the sum of the pixel intensity values. Five random fields were selected for each slide, and the green color intensity was averaged and the signal detected in the negative controls was subtracted from the average. HIF-1α abundance in the image is expressed as the sum of green pixel intensity $\times 10^6/0.037$ mm^2.

Western blot analysis of MAPK. The cytosolic and nuclear protein extracts were obtained following published protocols (12, 13). Frozen tissue was homogenized in lysis buffer solution (10 m*M* Hepes, 10 m*M* KCl, 0.1 m*M* EDTA, 0.1 m*M* EGTA, 1 m*M* dithiothreitol [DTT], 0.5% Triton X-100, 0.5 m*M* phenylmethylsulfonyl fluoride [PMSF], 1 m*M* sodium orthovanadate, 10 m*M* β-glycerophosphate, and 50 m*M* NaF) containing Protease Inhibitor Cocktail (Roche, Mannheim, Germany). After incubation on ice (10 mins), nuclear and cytosolic proteins were separated by centrifugation (1000 *g*, 4°C, 5 mins). Supernatant containing cytosolic proteins was transferred to a precooled microcentrifuge tube, frozen in liquid nitrogen, and stored at –80°C. The pellet was incubated (4°C, 1 hr) in lysis buffer solution (20 m*M* Hepes, 400 m*M* NaCl, 1 m*M* EDTA, 1 m*M* EGTA, 1 m*M* DTT, 1 m*M* PMSF, 1 m*M* sodium orthovanadate, 10 m*M* β-glycerophosphate, 50 m*M* NaF, and protease inhibitors). After centrifugation (10,000 *g*, 4°C, 15 mins), the supernatant containing nuclear proteins was transferred to a cold microcentrifuge tube, frozen in liquid nitrogen, and stored at –80°C. Total protein in each fraction was measured by a modified Lowry assay using bovine serum albumin as a standard. The purity of cytosolic and nuclear fractions was evaluated by measuring typical subcellular markers by Western blot: to assess the purity of the cytosolic fraction, we verified the presence of β-actin and the absence of histone deacetylase-1, whereas the purity of the nuclear fraction was assessed by verifying the presence of histone deacetylase-1 and the absence of β-actin, as suggested (13).

The protein extracts were used for sodium dodecyl sulfate–polyacrylamide gel electrophoresis Western blot as follows. Proteins (≈80 μg) from either the cytosolic or the nuclear fraction were heated at 95°C for 5 mins, followed by electrophoresis on a 12% denaturing gel and electroblotting onto nitrocellulose membranes. Loading of equal amounts of each MAPK protein for each tissue sample was verified by the intensities of the bands obtained with non–phospho-specific antibodies for ERK1/2 and p38. Membranes were incubated with 5% nonfat dry milk in TBS-Tween buffer (1 hr), followed by primary antibody (1:1000, 4°C, overnight)

and horseradish peroxidase–conjugated secondary antibody (1:2000, room temperature, 1 hr). Phosphorylated ERK1/2 and p38 protein levels were determined with phospho-specific antibodies (Cell Signaling Technology, Danvers, MA) that recognize phospho-ERK1/2 (Thr202/Tyr204) or phospho-p38 (Thr180/Tyr182). Immunoblots were developed using a chemiluminescent system (LumiGlo reagent/peroxide; Cell Signaling Technology). Band intensities were quantified with the National Institutes of Health AutoExtractor-1.51 software (Bethesda, MD). An extract from one normoxic heart was loaded on all blots for quantitative comparisons between blots. Data were normalized to normoxic controls and shown as fold-increases over normoxic levels.

For the determination of JNK activity, we measured the phosphorylation of c-Jun, a substrate of JNK. To this purpose, 100 μg tissue extract was incubated at room temperature for 1 hr with 1 μg glutathione *S*-transferase (GST)–c-Jun coupled with glutathione beads. After centrifugation (10,000 *g*, 1 min), the supernatant was removed, and the beads washed twice. Beads were resuspended (30°C, 30 mins) in 20 μl kinase buffer solution (20 m*M* Hepes, 20 m*M* β-glycerophosphate, 10 m*M* $MgCl_2$, and 1 m*M* DTT, pH 7.5) containing 1 μl [γ-^{33}P]ATP (3000 ci/mmol; Amersham, Piscataway, NJ). Samples were heated at 95°C for 5 mins, followed by electrophoresis on a 12% denaturating gel. Phosphorylated c-jun was resolved by autoradiography. Band intensities were analyzed as described above.

Inhibition of p38. The inhibitory effect of SB202190 on p38 activity was tested by measuring the phosphorylation of HSP27, a target of p38, by Western blot techniques using an anti–phospho-HSP27 antibody (Santa Cruz Biotechnology, Santa Cruz, CA). Loading of equal amounts of protein for each sample was verified by the intensities of bands obtained with non–phospho-specific antibodies for HSP27. Immunoblots were developed and analyzed as described above.

Statistics. All data are expressed as mean ± SE. To assess the significance of the differences, we first performed one-way ANOVA. If significant ($P < 0.05$), ANOVA was followed by the Dunnett's multiple comparison test. When two groups were compared, the Student's *t* test was used.

Results

When the hypoxic chamber was flowed with low-O_2 gas, the O_2 tension inside the chamber, monitored by an O_2 electrode, fell to 70–72 mm Hg within 10 mins after flow start. Thus, the effective duration of hypoxia in the "1-hr hypoxia" group was 50 mins. As all animals survived the experimental protocols, all data were admitted to statistical analysis.

HIF-1α Response to *In Vivo* Hypoxia and Reoxygenation. Figure 1A shows representative images of HIF-1α immunoperoxidase staining and immunofluorescence. One-hour hypoxia markedly increased HIF-1α signal, which did not increase further in the next 23 hrs. For the reoxygenation, the hypoxic chamber was opened, which led the O_2 tension inside the chamber to return to atmospheric in <1 min. The reoxygenation decreased the HIF-1α signal to the baseline value.

To detect differences among the various conditions, we performed a quantitative estimate of HIF-1α from the immunofluorescence images obtained for all animals by calculating the total green pixel intensity per unit area (Fig. 1B) as previously described (9, 11). As the variance of pooled data by one-way ANOVA yielded $P < 0.0001$, we assumed that the variation among the means was greater than that expected by chance alone, thereby enabling the Dunnett post-test. Figure 1B confirms that the HIF-1α signal is acutely increased after 1-hr hypoxia, remains constant for 23 hrs, and is quickly blunted after the reoxygenation. Figure 1C reports a representative Western blot of a 1-hr hypoxia sample to show the specificity of the primary anti–HIF-1α antibody.

***In Vivo* Hypoxia and MAPK Signaling.** We measured ERK1/2 and p38 both as total and phosphorylated proteins by Western blot techniques, as well as JNK activity as the rate of c-Jun phosphorylation. As these measurements were performed in both the nuclear and cytosolic fractions, we first assessed whether the changes in nuclear and cytosolic values were related (Fig. 2). To this purpose, the insets in Figure 2, which represent the respective protein abundances in the cytosolic and nuclear extracts after 1-hr hypoxia (left and right, respectively) in a representative sample, show that the two measurements are highly related. To add statistical consistency, we linearly correlated all the pairs (nuclear vs. cytosolic) obtained in this study separately for each protein. The correlation excluded measurable deviations in the nuclear or cytosolic localization of these proteins, thereby enabling us to take the cytosol measurements as representative of the situation in the nuclei and in the whole cell.

Then, we assessed whether total ERK1/2 and total p38 protein levels responded to hypoxia and reoxygenation. Because the total protein level remained unaffected (Fig. 3A), we considered only the changes in the phosphorylated forms of ERK1/2 (Phospho-ERK1/2) and p38 (Phospho-p38).

Finally, we determined the response of Phospho-ERK1/2 and Phospho-p38 protein levels, as well as JNK activity during hypoxia followed by reoxygenation (Fig. 3B). The quantitative densitometry of the blots, expressed as fold increase over normoxia, showed that Phospho-ERK1/2 did not respond, remaining close to the normoxia value. By contrast with ERK1/2, Phospho-p38 increased transiently after 1-hr hypoxia but declined to near normoxic levels after 23-hr hypoxia. The reoxygenation did not further change Phospho-p38. The JNK kinase activity responded quickly to hypoxia but remained sustained through hypoxia reoxygenation.

Selective Inhibition of p38 Activity. To assess the

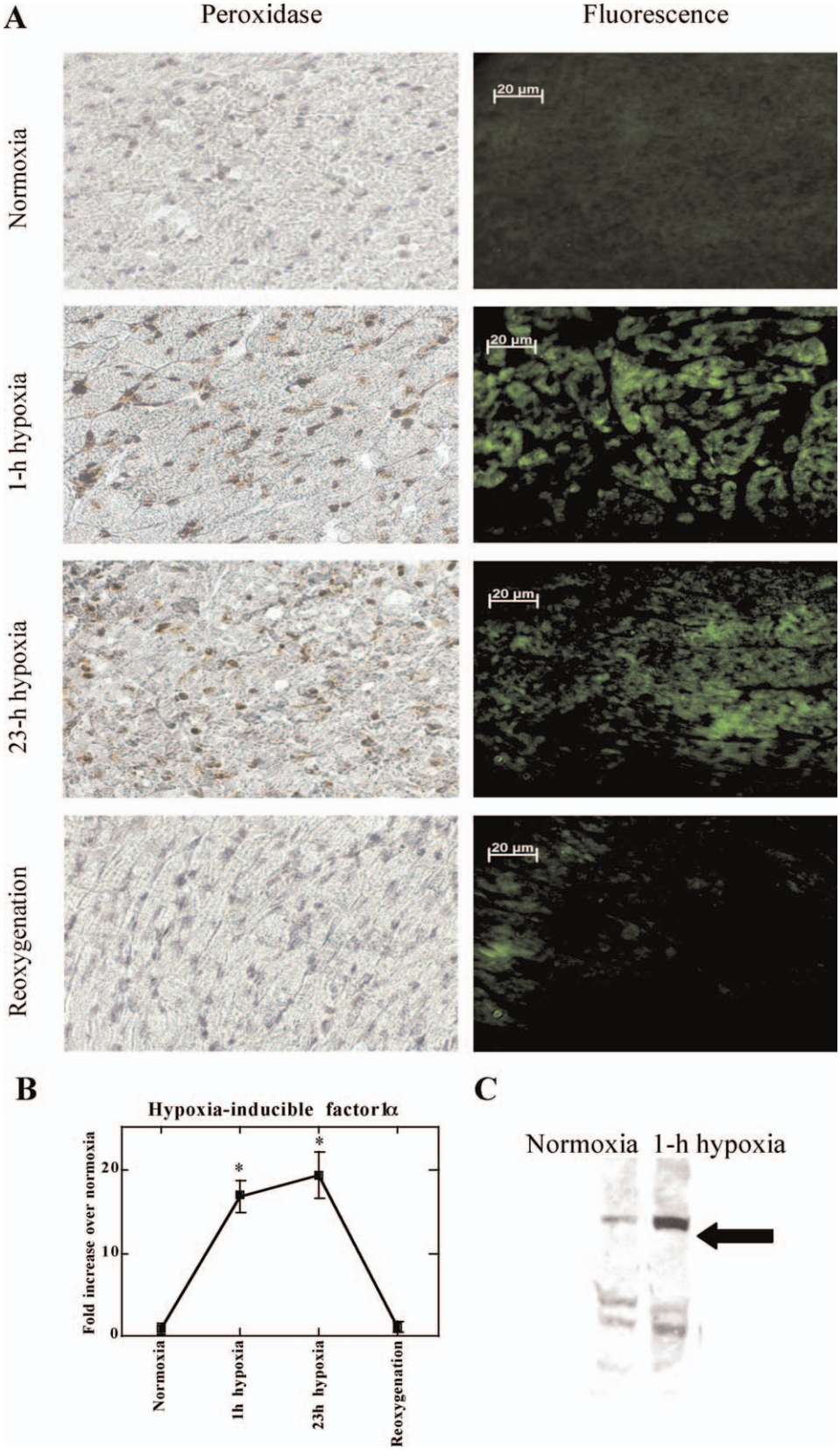

Figure 1. (A) Representative images taken from left ventricle biopsies during the hypoxia reoxygenation protocol. The left and right columns show HIF-1α immunoperoxidase staining, with HIF-1α giving brown spots, and HIF-1α immunofluorescence staining, with HIF-1α giving a green signal, respectively. The horizontal bars in the fluorescence column mark 20 μm, with the pictures in the peroxidase column at the same magnification. (B) Quantification of the immunofluorescence staining, expressed as the increase of the intensity of green pixels over the value

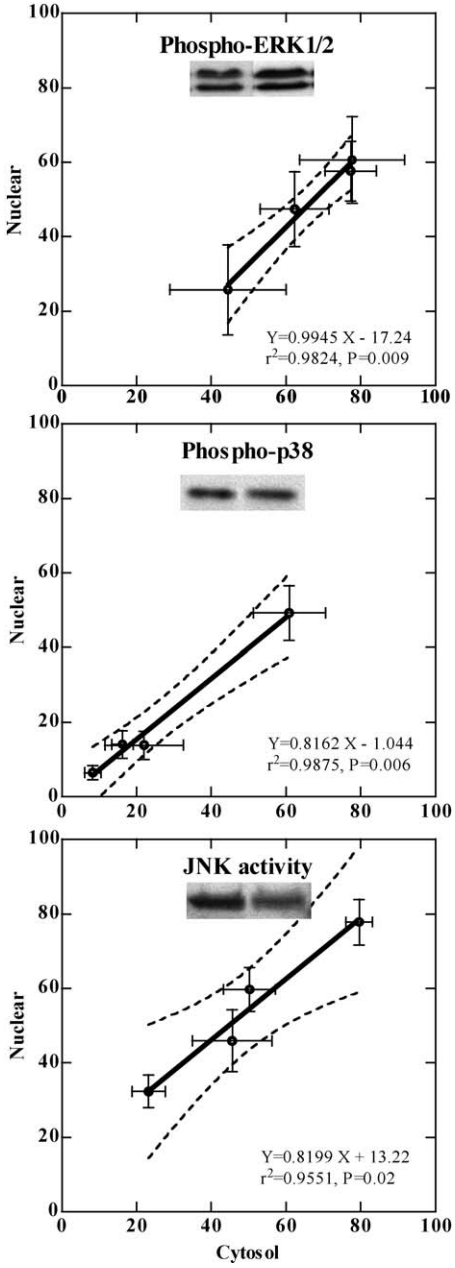

Figure 2. Relationship between the cytosolic and nuclear abundance of (from top to bottom) Phospho-ERK1/2, Phospho-p38, and JNK activities. Each panel reports the blots showing the respective protein abundance in the cytosolic and nuclear extracts after 1-hr hypoxia (left and right, respectively) in a representative sample. The linear regression obtained using all the available pairs is reported, along with the 95% confidence bands. The insets in the bottom report the equation of the best fit, with the value of the correlation coefficient (r^2) and *P*. Each point represents mean ± SE. Population (*n*) is the same as in Figure 1.

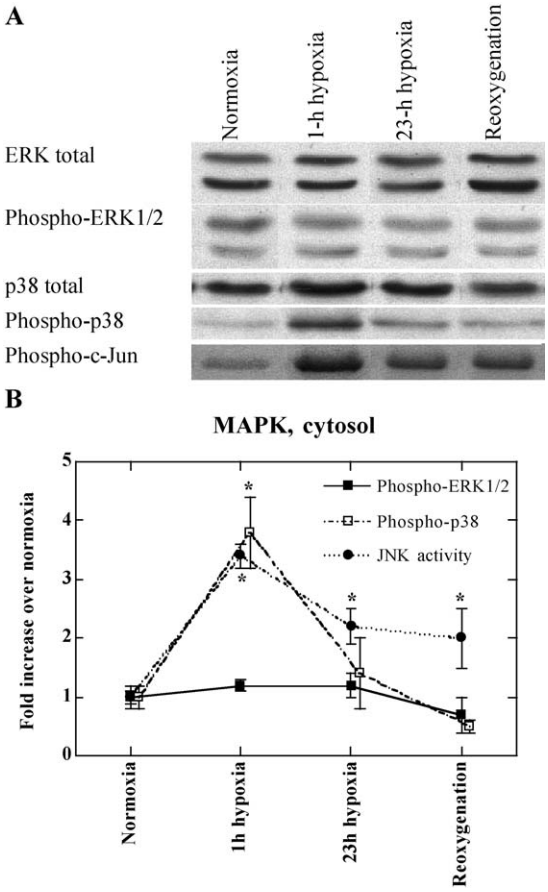

Figure 3. (A) Representative Western blot analysis of total ERK1/2, Phospho-ERK1/2, total p38, Phospho-p38, and Phospho-c-Jun, a marker of JNK activity. Each marker was measured in normoxia, during hypoxia (1 and 23 hrs) and after reoxygenation. (B) Average densitometric analysis (mean ± SE) of the blots obtained for all animals is expressed as fold increase over normoxia for the expression level of Phospho-ERK1/2, Phospho-p38 and Phospho-c-Jun, or JNK activity. One-way ANOVA *P* was NS, 0.0009, 0.02, and 0.0001, respectively. When ANOVA $P < 0.05$, the Dunnett test was performed *versus* normoxia (*). Population (*n*) is the same as in Figure 1.

involvement of the p38 path during acute hypoxia, we treated a group of rats with SB202190, an inhibitor of the p38 function (8). The drug was administered just before hypoxia, which lasted 1 hr in order to ensure persisting activity of SB202190 during hypoxia. To assess the efficacy of the inhibition, we measured a known target of p38 (e.g., phosphorylated HSP27), which was reduced by one half with respect to hypoxia without SB202190 (Fig. 4A), indicating that the drug selectively inhibited the action of p38. The inhibition was accompanied by a marked reduction in HIF-1α (Fig. 4B). To add statistical consistency (Fig. 4C), we averaged the fold increase over normoxia from

←
measured during normoxia in all animals (mean ± SE, $n = 6, 6, 6$, and 4 for normoxia, 1-hr hypoxia, 23-hr hypoxia, and reoxygenation, respectively). One-way ANOVA $P < 0.0001$. *$P < 0.05$ (Dunnett post-test) *versus* normoxia. (C) Representative Western blot of a 1-hr hypoxia sample to show the specificity of the primary anti–HIF-1α antibody. The arrow indicates the position of the 116-kDa molecular weight marker. Color figure available in the online version of the journal.

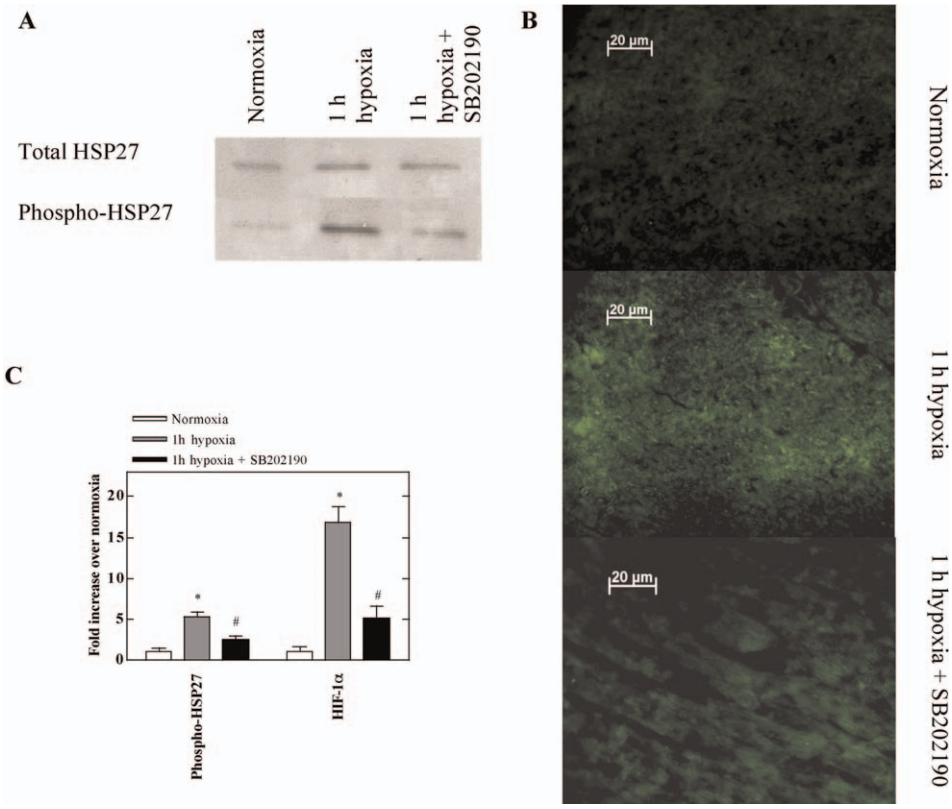

Figure 4. Selective inhibition of p38 action with SB202190 given prior to hypoxia. (A) Representative Western blots of a known target of p38 (i.e., phospho-HSP27). (B) Representative images taken from left ventricle biopsies before and after 1-hr hypoxia, with and without added SB202190, with HIF-1α giving a green signal. The horizontal bars mark 20 μm. (C) Quantitative analysis of Phospho-HSP27 and HIF-1α at the end of 1-hr hypoxia with and without SB202190 ($n = 6$, 6, and 4 for normoxia, 1-hr hypoxia and 1-hr hypoxia with SB202190, respectively). One-way ANOVA $P = 0.001$ and $P < 0.0001$, respectively. *$P < 0.05$ *versus* normoxia; #$P < 0.05$ *versus* 1-hr hypoxia without SB202190. Color figure available in the online version of the journal.

either blot densitometry (phosphorylated HSP27) or the sum of green pixel intensity, which was obtained as described above (HIF-1α).

Discussion

The strategy selected to test the hypotheses at the basis of this study (i.e., that HIF-1α overexpression occurs in the hypoxic myocardium *in vivo* and that MAPK signaling is associated with HIF-1α) made use of a rodent model of hypoxia, with measurement of the expression of various proteins at appropriate times during 23-hr hypoxia followed by reoxygenation. Some of the measured parameters, with special concern to HIF-1α, are time sensitive and O_2 sensitive. Therefore, when hypoxic data were needed, we anesthetized and sacrificed the animals under hypoxic conditions, thereby preventing the reoxygenation of hypoxic tissue by a procedure that resulted in consistently raised levels of HIF-1α and related proteins (11).

The observed fast HIF-1α increase within 1 hr after the onset of hypoxia is consistent with the view that hypoxia does not affect the synthesis of HIF-1α, a rapid turnover protein, but rather its stabilization (14). Reoxygenation of the hypoxic myocardium returned HIF-1α to the normoxic value, in agreement with the short (few minutes) $t_{1/2}$ of HIF-1α measured in reoxygenated cell cultures (15) and mouse brain (16).

The activation of the p38 and JNK paths in acute hypoxia is consistent with data obtained in cultured cardiac myocytes (17), isolated perfused hearts (18), and mouse and pig hearts *in vivo* (19). Furthermore, hypoxic (1% O_2 for 16 hrs) Hep3B and HEK293 cells induced p38 activity in a Rac1-dependent manner (6). In adult cardiac myocytes, acute (5–10 mins) exposure to 2,4-dinitrophenol rapidly activates adenosine 5′-monophosphate–activated protein kinase (AMPK) and p38 (20). The present study points to a link between p38 and HIF-1α *in vivo* that is suggestive, because the involvement of p38 in O_2 sensing meets many criteria of hypoxia response. First, although the existence of hypoxia-induced reactive O_2 species (ROS) is controversial, it appears that in skeletal muscle, but also in myocardial tissue, a small but significant ROS signal is produced during exposure to hypoxia that may be within the range of normal physiologic or mildly pathophysiologic signaling mechanisms (21). Although the molecular and intracellular origins of the ROS signal are unknown, mitochondria appear to be involved, based on studies done in hearts and in isolated cells (22). Another controversial matter is whether ROS are essential to trigger the p38 pathway. However, ROS were

shown to activate MAPK by a variety of mechanisms, including oxidation of active cysteinyl residues, involvement of protein kinase C or the apoptosis signal-regulating kinase 1, and activation of the guanine nucleotide-binding protein Ras (23). In amphibian hearts, p38 is activated by ROS generated from xanthine/xanthine oxidase but is suppressed by catalase and superoxide dismutase (24). Finally, it was shown in adult cardiac myocytes that p38 is activated by chemical hypoxia via AMPK (20), a key sensor of the cell energy status and a hallmark of hypoxia (25). Although this mechanism needs further validation, these observations converge in indicating that hypoxia may activate the p38 pathway, either *via* ROS or *via* low cell energy status.

The occurrence of mechanisms alternative to proline hydroxylation to regulate HIF-1α activity bypasses both the problem constituted by the high value for the Michaelis-Menten constant for O_2 in the hydroxylation reaction (4) and the assignment of a specific role to mitochondrial ROS. We did not observe appreciable changes in ERK1/2 signaling during *in vivo* hypoxia, in contrast with observations obtained *in vitro* (26) and in neonatal rat brain (27). Despite comparable degrees of hypoxia, it would not be surprising if the paths related to ERK signaling differed in brain and myocardium (9).

The correlation between p38 activation and HIF-1α accumulation is clear only during the first hour of hypoxia; afterward, HIF-1α continues to be stabilized for at least 23 hrs, whereas p38 activation decreases faster. This unexplained finding needs to be assessed in future work based on a more detailed kinetics of the changes in p38 and HIF-1α during the first 23 hrs of hypoxia in order to further analyze proline hydroxylation of HIF-1α downstream of p38 activation. However, this study shows that p38 activation is linked to HIF-1α accumulation during *in vivo* hypoxia in the heart, which may provide clues to understanding the hypoxic signaling mechanism at a physiologic level in models other than those from cells cultured *in vitro*.

Conclusions. The purposes of this study were: (1) to investigate the dynamics of HIF-1α during *in vivo* hypoxia in the myocardium, a situation for which there is little support for HIF-1α overexpression, and (2) to test the association between MAPK and HIF-1α *in vivo*. Comparative examination of the MAPK and HIF-1α signaling pathways in the *in vivo* myocardium in rats exposed to hypoxia followed by reoxygenation indicated that: (a) the ERK1/2 pathway remained unaffected, (b) the p38 pathway was activated by acute hypoxia only, (c) the JNK pathway was higher than during normoxia, and (d) these changes are correlated with changes in HIF-1α, which was maximally stabilized after 1-hr hypoxia, and was destabilized upon reoxygenation.

1. Semenza G. HIF-1 and tumor progression: pathophysiology and therapeutics. Trends Mol Med 8:S62–S67, 2002.
2. Manalo DJ, Rowan A, Lavoie T, Natarajan L, Kelly BD, Ye SQ, Garcia JG, Semenza GL. Transcriptional regulation of vascular endothelial cell responses to hypoxia by HIF-1. Blood 105:659–669, 2005.
3. Jaakkola P, Mole D, Tian Y, Wilson M, Gielbert J, Gaskell S, von Kriegsheim A, Heberstreit H, Mukherji M, Schofield C, Maxwell P, Pugh C, Ratcliffe P. Targeting of HIFa to the von Hippel-Lindau ubiquitylation complex by O_2-regulated prolyl hydroxylation. Science 292:468–472, 2001.
4. Koivunen P, Hirsila M, Kivirikko KI, Myllyharju J. The length of peptide substrates has a marked effect on hydroxylation by the hypoxia-inducible factor prolyl 4-hydroxylases. J Biol Chem 281:28712–28720, 2006.
5. Berra E, Benizri E, Ginouves A, Volmat V, Roux D, Pouyssegur J. HIF prolyl-hydroxylase 2 is the key oxygen sensor setting low steady-state levels of HIF-1alpha in normoxia. EMBO J 22:4082–4090, 2003.
6. Hirota K, Semenza GL. Rac1 activity is required for the activation of hypoxia-inducible factor 1. J Biol Chem 276:21166–21172, 2001.
7. Emerling BM, Platanias LC, Black E, Nebreda AR, Davis RJ, Chandel NS. Mitochondrial reactive oxygen species activation of p38 mitogen-activated protein kinase is required for hypoxia signaling. Mol Cell Biol 25:4853–4862, 2005.
8. Karahashi H, Nagata K, Ishii K, Amano F. A selective inhibitor of p38 MAP kinase, SB202190, induced apoptotic cell death of a lipopolysaccharide-treated macrophage-like cell line, J774.1. Biochim Biophys Acta 1502:207–223, 2000.
9. Bianciardi P, Fantacci M, Caretti A, Ronchi R, Milano G, Morel S, von Segesser L, Corno A, Samaja M. Chronic in vivo hypoxia in various organs: hypoxia-inducible factor-1alpha and apoptosis. Biochem Biophys Res Commun 342:875–880, 2006.
10. Milano G, Corno A, Lippa S, von Segesser L, Samaja M. Chronic and intermittent hypoxia induce different degrees of myocardial tolerance to hypoxia-induced dysfunction. Exp Biol Med 227:389–397, 2002.
11. Fantacci M, Bianciardi P, Caretti A, Coleman TR, Cerami A, Brines M, Samaja M. Carbamylated erythropoietin ameliorates the metabolic stress induced in vivo by severe chronic hypoxia. Proc Natl Acad Sci U S A 103:17531–17536, 2006.
12. Morel S, Milano G, Ludunge KM, Corno AF, Samaja M, Fleury S, Bonny C, Kappenberger L, von Segesser LK, Vassalli G. Brief reoxygenation episodes during chronic hypoxia enhance posthypoxic recovery of LV function: role of mitogen-activated protein kinase signaling pathways. Basic Res Cardiol 101:336–345, 2006.
13. Fryer RM, Pratt PF, Hsu AK, Gross GJ. Differential activation of extracellular signal regulated kinase isoforms in preconditioning and opioid-induced cardioprotection. J Pharmacol Exp Ther 296:642–649, 2001.
14. Jewell U, Kvietikova I, Scheid A, Bauer C, Wenger R, Gassmann M. Induction of HIF-1alpha in response to hypoxia is instantaneous. FASEB J 15:1312–1314, 2001.
15. Jiang B, Semenza G, Bauer C, Marti H. Hypoxia-inducible factor 1 levels vary exponentially over a physiologically relevant range of O2 tension. Am J Physiol 271:C1172–C1180, 1996.
16. Stroka D, Burkhardt T, Desbaillets I, Wenger R, Neil D, Bauer C, Gassmann M, Candinas D. HIF-1 is expressed in normoxic tissue and displays an organ-specific regulation under systemic hypoxia. FASEB J 15:2445–2453, 2001.
17. Kulisz A, Chen N, Chandel N, Shao Z, Schumacker P. Mitochondrial ROS initiate phosphorylation of p38 MAP kinase during hypoxia in cardiomyocytes. Am J Physiol 282:L1324–L1329, 2002.
18. Yue T, Wang C, Gu J, Ma X, Kumar S, Lee J, Feuerstein G, Thomas H, Maleeff B, Ohlstein E. Inhibition of extracellular signal-regulated kinase enhances ischemia/reoxygenation-induced apoptosis in cultured cardiac myocytes and exaggerates reperfusion injury in isolated perfused heart. Circ Res 86:692–699, 2000.
19. Schulz R, Gres P, Skyschally A, Duschin A, Belosjorow S, Konietzka I, Heusch G. Ischemic preconditioning preserves connexin 43

phosphorylation during sustained ischemia in pig hearts in vivo. FASEB J 17:1355–1357, 2003.

20. Pelletier A, Joly E, Prentki M, Coderre L. Adenosine 5′-monophosphate-activated protein kinase and p38 mitogen-activated protein kinase participate in the stimulation of glucose uptake by dinitrophenol in adult cardiomyocytes. Endocrinology 146:2285–2294, 2005.
21. Clanton TL. Hypoxia induced reactive oxygen formation in skeletal muscle. J Appl Physiol (in press), 2007.
22. Guzy RD, Schumacker PT. Oxygen sensing by mitochondria at complex III: the paradox of increased reactive oxygen species during hypoxia. Exp Physiol 91:807–819, 2006.
23. Sugden PH, Clerk A. Oxidative stress and growth-regulating intracellular signaling pathways in cardiac myocytes. Antioxid Redox Signal 8:2111–2124, 2006.
24. Gaitanaki C, Papatriantafyllou M, Stathopoulou K, Beis I. Effects of various oxidants and antioxidants on the p38-MAPK signalling pathway in the perfused amphibian heart. Mol Cell Biochem 291: 107–117, 2006.
25. Hardie DG. Minireview: the AMP-activated protein kinase cascade: the key sensor of cellular energy status. Endocrinology 144:5179–5183, 2003.
26. Richard DE, Berra E, Gothie E, Roux D, Pouyssegur J. p42/p44 mitogen-activated protein kinases phosphorylate hypoxia-inducible factor 1alpha (HIF-1alpha) and enhance the transcriptional activity of HIF-1. J Biol Chem 274:32631–32637, 1999.
27. Jones NM, Bergeron M. Hypoxia-induced ischemic tolerance in neonatal rat brain involves enhanced ERK1/2 signaling. J Neurochem 89:157–167, 2004.